


**Enantioselectivity** Hot Paper

 How to cite: *Angew. Chem. Int. Ed.* **2023**, *62*, e202313606  
 doi.org/10.1002/anie.202313606

# Creating a Defined Chirality in Amino Acids and Cyclic Dipeptides by Photochemical Deracemization

Johannes Großkopf, Manuel Plaza, Roger Jan Kutta, Patrick Nuernberger, and Thorsten Bach\*

 Dedicated to Professor G. K. Surya Prakash on the occasion of his 70<sup>th</sup> birthday

**Abstract:** 2,5-Diketopiperazines are cyclic dipeptides displaying a wide range of applications. Their enantioselective preparation has now been found possible from the respective racemates by a photochemical deracemization (53 examples, 74 % to quantitative yield, 71–99 % *ee*). A chiral benzophenone catalyst in concert with irradiation at  $\lambda=366$  nm enables to establish the configuration at the stereogenic carbon atom C6 at will. If other stereogenic centers are present in the diketopiperazines they remain unaffected and a stereochemical editing is possible at a single position. Consecutive reactions, including the conversion into *N*-aryl or *N*-alkyl amino acids or the reduction to piperazines, occur without compromising the newly created stereogenic center. Transient absorption spectroscopy revealed that the benzophenone catalyst processes one enantiomer of the 2,5-diketopiperazines preferentially and enables a reversible hydrogen atom transfer that is responsible for the deracemization process. The remarkably long lifetime of the protonated ketyl radical implies a yet unprecedented mode of action.

## Introduction

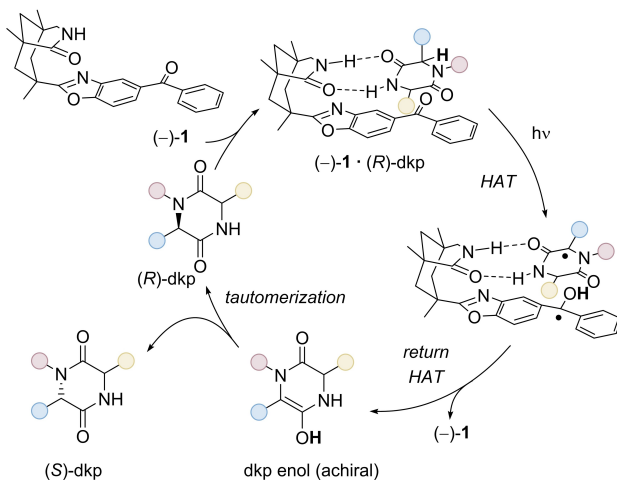
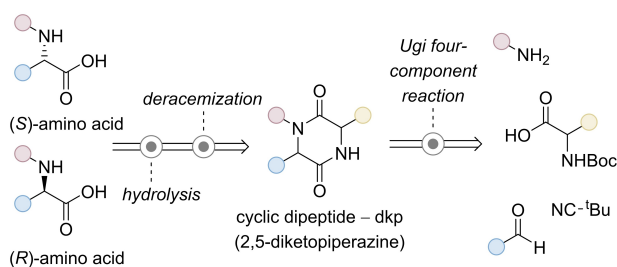
Chiral  $\alpha$ -amino acids represent quintessential molecular components for life on earth.<sup>[1]</sup> The exclusive occurrence of their (*S*)-enantiomers in nature has been a key topic in the

debate on the origins of chirality.<sup>[2]</sup> Apart from academic interest in the compounds, amino acids and their derivatives play a pivotal role as active ingredients in industry with sales valuing 26.1 billion US-\$ in 2021.<sup>[3]</sup> Among all amino acid derivatives, cyclic dipeptides (2,5-dkp=2,5-diketopiperazine) have emerged as one of the most important and versatile compound classes.<sup>[4,5]</sup> They display a plethora of pharmacological activities and can serve as precursors particularly for *N*-substituted but also for unsubstituted, enantiopure amino acids. Existing stereogenic centers within the dkp core can be favorably used to set up stereogenic centers in the periphery, e.g., by hydrogenation reactions.<sup>[6]</sup> Typically, enantiopure 2,5-dkps are prepared by an enantioselective reaction or by cyclizing dipeptides of enantiopure amino acids.<sup>[4]</sup> The separation<sup>[7]</sup> and resolution<sup>[8]</sup> of racemic chiral dkps represent viable options to access the compounds in enantiopure form although they deliver only a maximum of 50 % of the desired enantiomer. Photochemical deracemization is a conceivable alternative pathway to enantiopure dkps that starts from racemic material converting it quantitatively into a single enantiomer. In fact, the latter method<sup>[9–11]</sup> has recently been developed as a powerful tool for the light-induced, stoichiometric conversion of a racemic compound mixture into the same compound with a defined chirality. The key feature of the process is the combination of a photochemical step and a decoupled thermal step which intrinsically occur along different reaction channels. The first half reaction leads to a short-lived achiral intermediate which subsequently reacts in a consecutive thermal reaction, thus, overcoming the restrictions of microscopic reversibility.<sup>[12]</sup> Although other deracemization processes have been reported,<sup>[13]</sup> the photochemical approach<sup>[14]</sup> is particularly appealing due to its operational simplicity and its synthetic potential. Mechanistically, it has been shown that photochemical deracemization can be accomplished by a chiral catalyst that accounts for a differentiation in the photochemical event,<sup>[9,15–18]</sup> in the thermal event<sup>[19–22]</sup> or in both.<sup>[23]</sup> Focusing on photochemical deracemization reactions with a single photocatalyst, we have recently discovered that a selective hydrogen atom transfer (HAT) induced by a photoexcited chiral benzophenone offers a unique pathway for the deracemization at ubiquitous sp<sup>3</sup>-stereogenic carbon centers displaying a C–H bond.<sup>[24,25]</sup> We envisioned the method to be suitable for the preparation of enantiomerically pure dkps that can serve as precursors to a variety of amino acids (Scheme 1).

[\*] Dr. J. Großkopf, Dr. M. Plaza, Prof. Dr. T. Bach  
 Department Chemie and Catalysis Research Center (CRC),  
 School of Natural Sciences  
 Technische Universität München  
 D-85747 Garching (Germany)  
 E-mail: thorsten.bach@ch.tum.de

Dr. R. J. Kutta, Prof. Dr. P. Nuernberger  
 Institut für Physikalische und Theoretische Chemie,  
 Universität Regensburg  
 Universitätsstr. 31, D-93053 Regensburg (Germany)

© 2023 The Authors. *Angewandte Chemie International Edition* published by Wiley-VCH GmbH. This is an open access article under the terms of the Creative Commons Attribution Non-Commercial License, which permits use, distribution and reproduction in any medium, provided the original work is properly cited and is not used for commercial purposes.



**Scheme 1.** Chiral amino acids and 2,5-diketopiperazines (2,5-dkps) are accessible from simple starting compounds by an Ugi reaction (top). Putative reaction pathway for the deracemization of a dkp by catalyst (-)-1 leading to (S)-diketopiperazines and (S)-amino acids. The enantiomeric (R)-products would be available with the enantiomeric catalyst (+)-1 (bottom). For a more comprehensive discussion of the mechanism, the reader is referred to the final sections of the manuscript.

Racemic 2,5-dkps can be rapidly assembled by an Ugi-four-component reaction<sup>[26]</sup> and their respective enantiomers were expected to display different reactivity in the complex with the chiral benzophenone catalyst (-)-1. Upon photoexcitation, benzophenones are known to undergo a HAT from aliphatic C–H bonds to their oxygen atom.<sup>[27,28]</sup> Within complex (-)-1·(R)-dkp, the HAT is geometrically feasible and should deliver a planar dkp-based, carbon-centered radical and a protonated ketyl radical derived from (-)-1. Rapid return HAT would lead to regeneration of the catalyst and to formation of an achiral dkp enol which tautomerizes to both dkp enantiomers. Based on our previous work,<sup>[25,29]</sup> we anticipated that enantiomer (S)-dkp would not be processed by the catalyst and, thus, would be enriched in the reaction medium. If enantiomeric (R)-dkp and the respective (R)-amino acids were required, the enantiomeric catalyst (+)-1 was to be used. Herein, we report the successful implementation of this strategy for the deracemization of a wide range of 2,5-dkps. Full details on possible applications of the enantioenriched products and on the identification of deracemization intermediates by transient absorption spectroscopy are presented. The latter study revealed that both, the forward and the return HAT

step, are significantly slower than for the previously studied hydantoins.<sup>[25]</sup> The preferred HAT within complex (-)-1·(R)-dkp was confirmed, but a dkp-derived enol intermediate could not be detected.

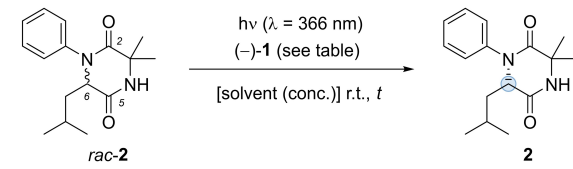
## Results and Discussion

Preliminary experiments were performed with a 2,5-dkp that displayed a stereogenic center at carbon atom C6. In this case, a single stereogenic center is edited by the deracemization process and the success of the reaction can be nicely monitored by the enantiomeric excess (*ee*) of the product. Furthermore, compounds of this type appeared to be promising precursors which allow access to *N*-substituted amino acid and other biologically active compounds (see below). Compound *rac-2* was readily assembled from commercially available isovaleraldehyde, *tert*-butylisocyanide, aniline, and *N-tert*-butyloxy(Boc)-protected  $\alpha$ -methylalanine in an Ugi reaction.<sup>[30]</sup>

The primary Ugi product was cyclized after deprotection and delivered the desired dkp upon hydrolysis (see Supporting Information for details). Initial photochemical experiments were performed with a substrate concentration of  $c = 2.5$  mM and with benzophenone (-)-1 as catalyst (5 mol %). Experiments using dichloromethane (Table 1, entry 1) and acetonitrile (entry 2) as solvents were not promising as they delivered, if any, only a negligible enantioselectivity for product **2** after 13 hours of irradiation ( $\lambda = 366$  nm). The low-polarity solvent trifluorotoluene was required to guarantee for a significant differentiation between the two enantiomers resulting in the quantitative isolation of product **2** in 87% *ee* (entry 3). An increase in concentration was detrimental for both yield and enantioselectivity (entries 4 and 5) while a further decrease seemed undesirable from a preparative point of view. A decrease in catalyst loading led to a diminished selectivity (entry 6). Its increase, however, resulted in an improved enantioselectivity (93% *ee*) without compromising the yield (entry 7). The *ee* was monitored over time (see the Supporting Information), indicating that the deracemization was complete after 13 hours. This notion was confirmed by performing the reaction for 16 hours (entry 8). Further modifications regarding the reaction temperature (entry 9) and the irradiation wavelength (entry 10) did not lead to a better performance, establishing the conditions of entry 7 as best suited for further studies. For all reactions, the exclusion of molecular oxygen was crucial to attain a rapid and clean conversion.

The photochemical deracemization protocol was applied to a range of 2,5-dkps (Scheme 2). A first set of substrates (*rac-3* to *rac-32*) displayed a phenyl group at nitrogen atom N1 and a single stereogenic center at carbon atom C6. A defined configuration at this stereogenic center was consistently created upon irradiation at  $\lambda = 366$  nm in the presence of catalyst (-)-1. The absolute configuration was proven to be (S) by hydrolysis of representative dkps to their  $\alpha$ -amino acids (see below) and comparison with authentic material derived from commercially available (S)-amino acids (phenylalanine and leucine). The size of the substituent at the

**Table 1:** Optimization of reaction conditions for the 6-isobutyl-substituted 2,5-dkp *rac-2*. The reactions were performed by irradiation of the sample for the indicated time period (*t*) with an external light source (fluorescent lamps with  $\lambda$  given as emission maximum) at room temperature (r.t.) in degassed solution.



Entry <sup>[a]</sup>	Solvent	c [mM]	<b>2</b> [mol %]	Time [h]	Yield <sup>[b]</sup> [%]	<i>ee</i> <sup>[c]</sup> [%]
1	CH <sub>2</sub> Cl <sub>2</sub>	2.5	5	13	quant.	0
2	MeCN	2.5	5	13	quant.	7
3	PhCF <sub>3</sub>	2.5	5	13	quant.	87
4	PhCF <sub>3</sub>	10	5	13	94	83
5	PhCF <sub>3</sub>	5	5	13	96	85
6	PhCF <sub>3</sub>	2.5	2.5	13	quant.	74
<b>7</b>	<b>PhCF<sub>3</sub></b>	<b>2.5</b>	<b>10</b>	<b>13</b>	<b>97</b>	<b>93</b>
8	PhCF <sub>3</sub>	2.5	10	16	95	93
9 <sup>[d]</sup>	PhCF <sub>3</sub>	2.5	10	13	95	82
10 <sup>[e]</sup>	PhCF <sub>3</sub>	2.5	10	13	84	82

[a] Optimization experiments were conducted on a 25  $\mu$ mol scale under the indicated conditions at room temperature (25 °C) in a photoreactor. Irradiation was performed with light sources displaying an emission maximum at  $\lambda = 366$  nm (350–400 nm; see Supporting Information for additional information). [b] Yield of isolated product after chromatography. [c] Enantiomeric excesses (*ee*) were determined by HPLC on a chiral stationary phase. [d] The reaction was conducted at 0 °C. [e] Irradiation was performed with light sources displaying an emission maximum at  $\lambda = 350$  nm (300–400 nm; see the Supporting Information for details).

stereogenic center was not relevant for the outcome of the reaction, and even the alanine-derivative **7** was obtained in 87 % yield and 94 % *ee* (for exceptions, see the discussion below). Functional groups were tolerated as long as they did not interfere with the photoexcited benzophenone, e.g., by oxidation. Examples include cyclopropanes (products **3**, **19**, **21**, **26**), esters (product **5**), trifluoromethyl groups (products **13**, **14**, **16**, **29**), aryl halides (products **6**, **15**, **26**, **32**), ethers (products **16**, **23–25**), boronates (product **18**) and alkynes (products **23**, **25**). The dialkyl substitution pattern at C3 had no influence on the enantioselectivity for the alanine derivative (product **7** vs. **8**), for the leucine-derived dkps it led to a minimal deterioration of the product enantiopurity (product **2** vs. products **19**, **20**, **24**).

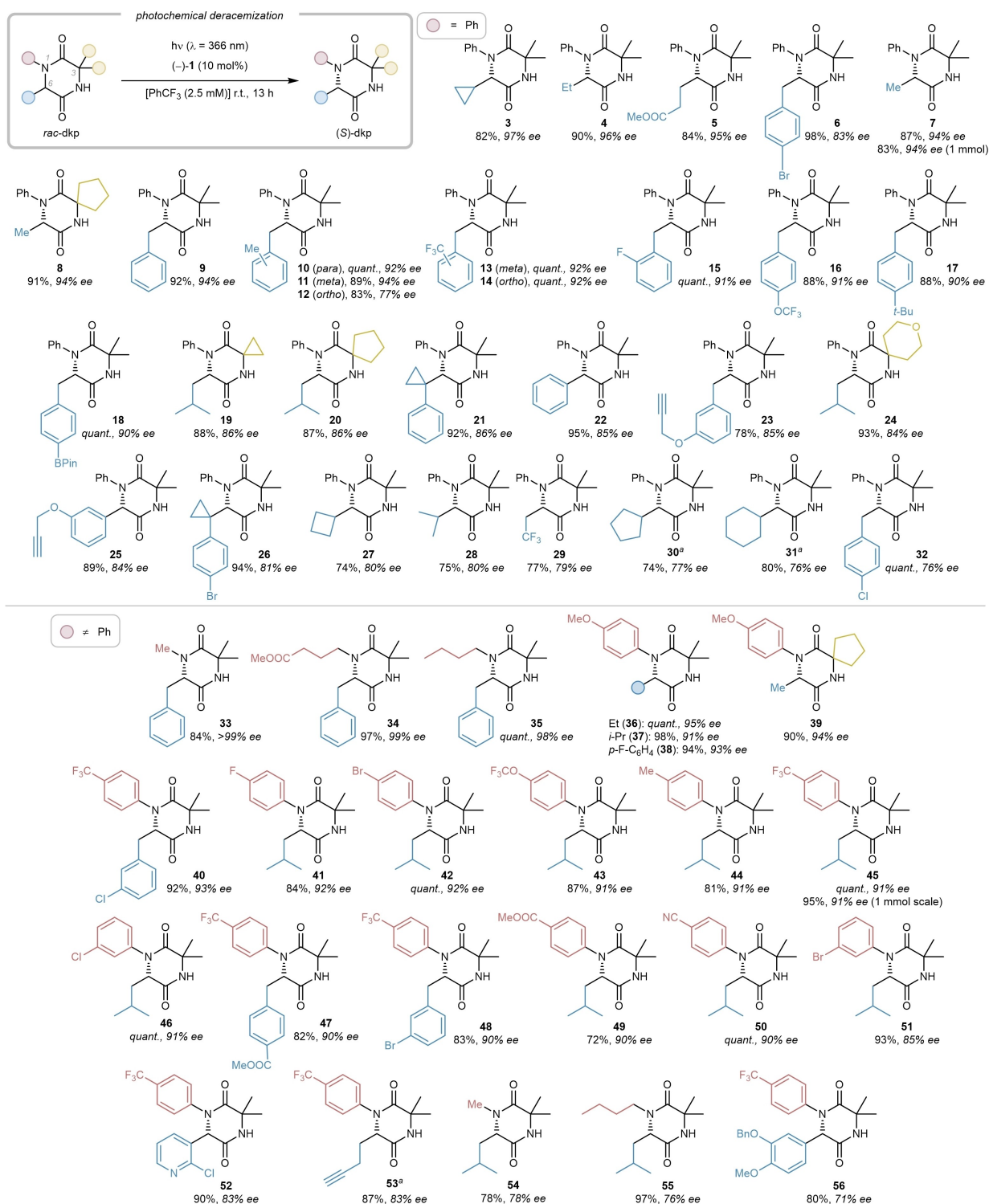
The stability of benzophenones (+)-**1** or (–)-**1** turned out to be a critical aspect in all deracemization experiments. If hydrogen abstraction occurs at other positions besides the stereogenic center, a protonated ketyl radical appears to be formed irreversibly which in turn initiates side reactions. This effect is particularly pronounced for compounds displaying tertiary carbon atoms next to the stereogenic center (products **27**, **28**, **30**, **31**). In the complex with excited catalyst (–)-**1** (cf. Scheme 1), HAT is expected not only to occur from the desired C–H bond but also from an adjacent position. We estimate the bond dissociation energy (BDE) of C6–H in 2,5-dkp<sup>[31]</sup> as 370–380 kJ mol<sup>–1</sup> but photoexcited

benzophenone has been found to undergo HAT at even stronger bonds<sup>[25,32]</sup> such as tertiary C–H bonds (BDE  $\cong$  400 kJ mol<sup>–1</sup>). The hypothesis that catalyst degradation was responsible for low enantioselectivities in these instances was supported by the fact that catalyst addition and continued irradiation led to a significant improvement in *ee*. A second aspect relevant for the application of the photochemical deracemization protocol pertains to the kinetic availability of the hydrogen atom within the 2,5-dkp. Empirically, we found that compounds showing a nuclear Overhauser effect (NOE) between substituents at C6 and C3 are not amenable to deracemization. The most notable case is the 6-*tert*-butyl-substituted 2,5-dkp which did not react in the deracemization protocol. If the molecule is forced to adopt a boat conformation and if a planar conformation is not accessible (see Supporting Information for details, for a list of unsuitable substrates, and for a guideline to predict the potential of untested 2,5-dkps), we suspect that a HAT is impossible due to elongated distances between the benzophenone and the C6 hydrogen atom.

A variation of the substituents at N1 was mainly performed with dkps derived from leucine or phenylalanine (products **33–56**). *N*-Alkylated dkps **33–35** derived from phenylalanine were obtained in excellent yields and with high *ee*. The reaction of *N*-arylated dkps with functionalized aryl groups emphasized the high functional group tolerance of the reaction, and the enantioselectivity remained consistently at 90 % *ee* or above (products **36–50**). Very few other products **53–56** gave slightly lower selectivities, possibly because they suffer from catalyst degradation (product **53**) or from not fully optimal geometrical constraints (see above).

A second set of experiments was performed to establish the photochemical deracemization in a more complex setting and to display its suitability for selective stereochemical editing (Scheme 3). In contrast to other photochemical editing protocols at sp<sup>3</sup>-carbon centers, which aim at the formation of a specific diastereoisomer and which employ achiral catalysts under substrate control,<sup>[33–38]</sup> the present deracemization protocol allows for a selective editing at a single position within the dkp under strict control by the catalyst. Starting from the respective aldehydes, 2,5-dkps **57** and **58** were obtained by an Ugi reaction as a mixture of diastereoisomers. Irradiation in the presence of catalyst (–)-**1** enabled editing the stereogenic center at C6. The other stereogenic centers were unaffected and the (6*S*)-diastereoisomer was obtained as the major diastereoisomer. Since 2,5-dkps are useful precursors for the synthesis of  $\alpha$ -amino acids, it is desirable to install the stereogenic  $\alpha$ -carbon atom at will. Starting from 2,5-dkp **59** with an existing stereogenic center in the alkyl chain, the stereogenic center at carbon atom C6 was edited to its (*S*)-form with catalyst (–)-**1** and to its (*R*)-form with catalyst (+)-**1**. The former product is a derivative of L-homoisoleucin, the latter of D-allo-homoisoleucin.

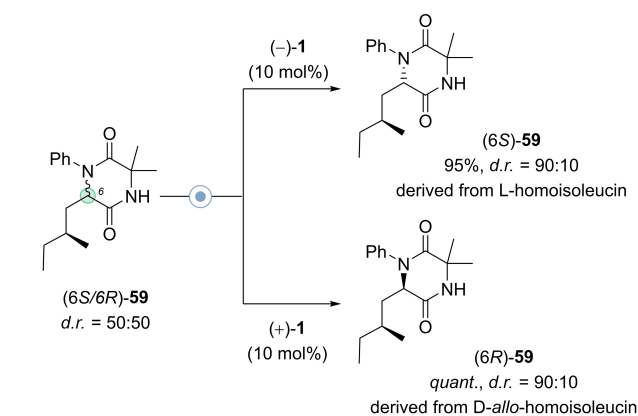
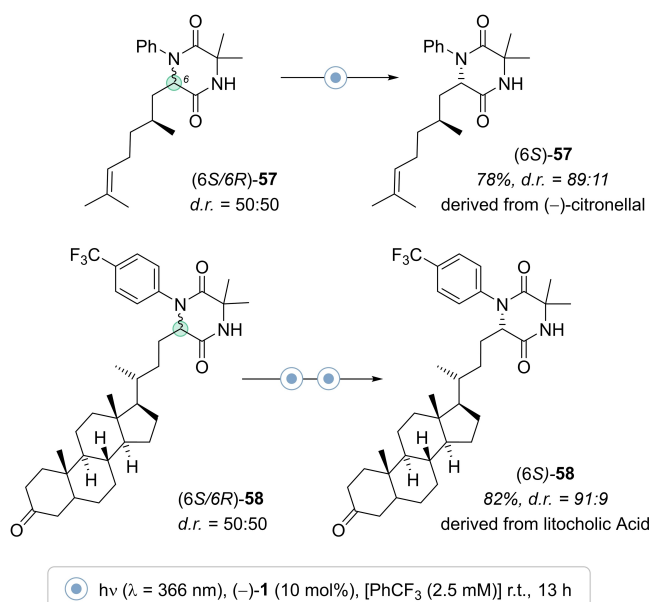
Beyond substrates with stereogenic centers at carbon atom C6, it was also shown that the stereogenic center at carbon atom C3 was affected by a photochemical deracemization. Despite the fact that the hydrogen atom at this



**Scheme 2.** Scope and limitations of the photochemical deracemization of 2,5-diketopiperazines (2,5-dkps) with a single stereogenic center at carbon atom C6 using chiral benzophenone (–)-1. Products in the upper section of the Scheme display a phenyl group at the nitrogen atom N1. Products in the lower section display various substituents at N1. All yields refer to isolated compounds (25 μmol scale) and the enantiomeric excess (*ee*) was determined by chiral HPLC analyses.

position may not be ideally oriented, a significant enrichment towards one enantiomer was observed (75% *ee*), the absolute configuration (3*S*) of which was assigned based on

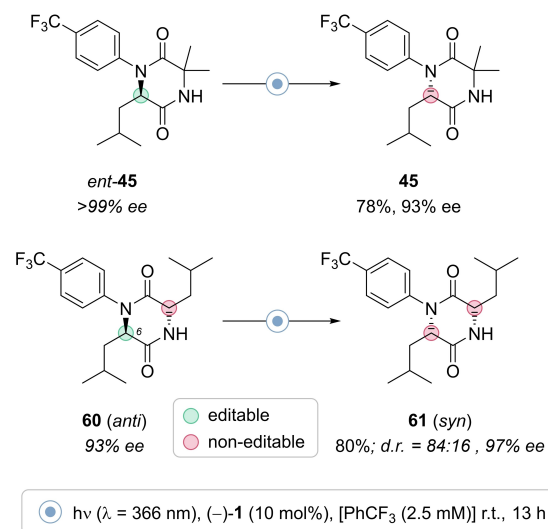
the depicted model for deracemization by catalyst (–)-1 (see the Supporting Information for details).



**Scheme 3.** Editing of natural product-derived dkps at C6 allows for a distinct product diastereoselectivity (top). The choice of catalyst enables the diastereoselective formation of homoisoleucin derivatives **59** (bottom) by adjusting the stereogenic center C6 at will.

If catalyst  $(-)\text{-1}$  does not decay by an unproductive HAT, it can perform several HAT cycles within a given deracemization reaction. The inversion of dkp  $\text{ent-45}^{[39]}$  (Scheme 4) requires every single substrate molecule to be processed at least once by the catalyst. The yield and the product *ee* for **45** testify that the catalyst is sufficiently robust to perform at least 7–8 turnovers, provided oxygen is strictly excluded. Stereogenic centers which already possess a configuration for which HAT is impossible in the complex with catalyst  $(-)\text{-1}$  will remain untouched, and their configuration is retained. In dkp *anti*-**60**, the stereogenic center at C3 displays already the (*S*)-configuration which is not further editable (see above), while the stereogenic center at C6 is editable. It is consequently possible to convert the *anti*-diastereoisomer **60** into the *syn*-diastereoisomer **61** by the photocatalytic deracemization protocol.

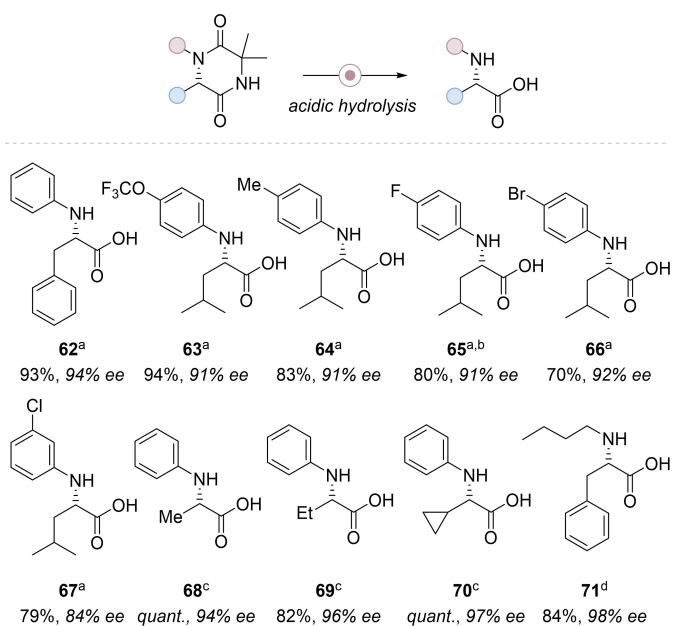
As pointed out in the introductory paragraph, 2,5-dkps can serve as versatile precursors for chiral  $\alpha$ -amino acids. Enantiopure *N*-arylamino acids are typically prepared by



**Scheme 4.** Inversion of configuration by a photochemical deracemization exemplified for the transformation  $\text{ent-45} \rightarrow \mathbf{45}$  and diastereoselective formation of dkp **61** by stereochemical editing at C6.

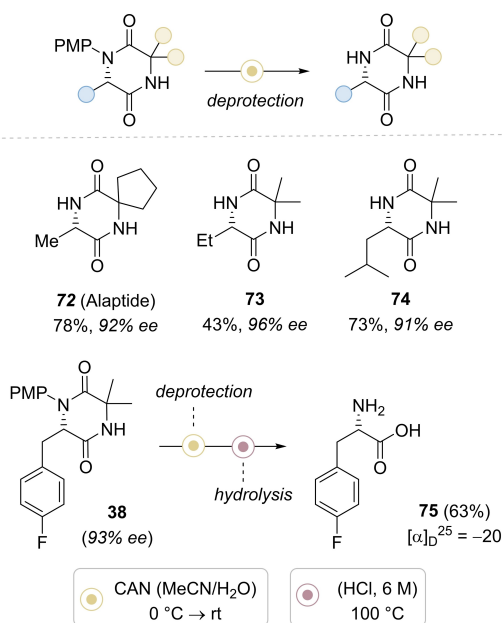
arylation of  $\alpha$ -amino acids, e.g., employing Buchwald–Hartwig conditions.<sup>[40]</sup> Since the starting material is chiral, it is mandatory to secure the configurational stability of the stereogenic center. Many arylation procedures require sophisticated reagents or alkaline conditions which hampers their applicability. Against this background, the 1-aryl-2,5-dkps, which are accessible by photochemical deracemization, represent excellent building blocks to access *N*-arylamino acids by straightforward acidic hydrolysis (Scheme 5). It was shown for a set of 2,5-dkps that the step, in nearly all cases (except for **67**), does not compromise the enantiopurity of the material and *N*-arylated amino acids **62–70** were obtained in high yields and *ee*. The same protocol was applied to 1-alkyl-2,5-dkp **35** leading to phenylalanine derivative **71**.

If the 1-aryl group of 2,5-dkps was *para*-methoxyphenyl (PMP), an oxidative deprotection became feasible, rendering an access to unprotected 2,5-dkps possible (Scheme 6). A prominent example is the 2,5-dkp alaptide for which several pharmacological activities have been reported<sup>[41]</sup> and which has found widespread applications in dermatology. The (*S*)-enantiomer **72** of alaptide was readily available from dkp **7** (Scheme 2) by treatment with ceric ammonium nitrate (CAN) in an acetonitrile/water mixture. Two additional unprotected diketopiperazines **73** and **74** were prepared employing the same cleavage conditions. The stereochemical integrity at carbon atom C6 was secured in the oxidation protocol. Taken together, the oxidative PMP cleavage and the dkp hydrolysis, serve to produce unprotected amino acids from 2,5-dkps. As an example, *para*-fluorophenylalanine (**75**) was synthesized starting from deracemization product **38** in 63% yield. The measured specific rotation ( $c = 0.94$ , H<sub>2</sub>O) does not perfectly match the literature value for the enantiopure compound ( $[\alpha]_D^{26} = -22$ ;  $c = 0.94$ , H<sub>2</sub>O)<sup>[42]</sup> but correlates well with the expected 93% *ee*.



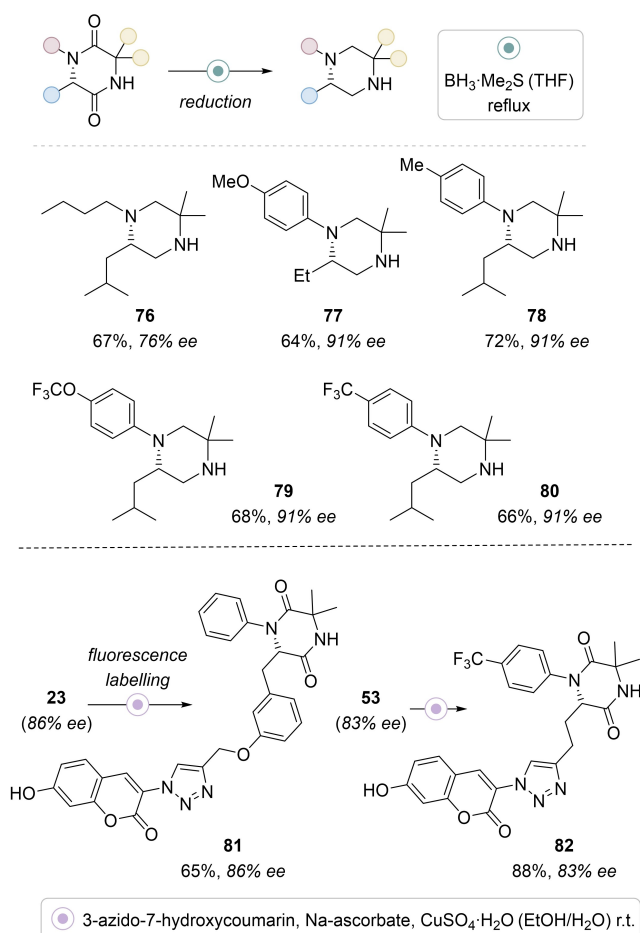
$\text{a}$ (HCl, 12 M) 100 °C.  $\text{b}$ 1 mmol scale.  $\text{c}$ (HCl, 6 M) 100 °C.  $\text{d}$ (HCl, 4 M) 100 °C.

**Scheme 5.** Preparation of *N*-arylated and *N*-alkylated  $\alpha$ -amino acids **62–71** by dkp hydrolysis under acidic conditions. The reactions proceed with complete retention of configuration (except for product **67**).



**Scheme 6.** Oxidative deprotection of the *para*-methoxyphenyl (PMP) group and complete deprotection of a 2,5-dkp to amino acid **75**.

Consecutive reactions of 2,5-dkps include a complete reduction to the saturated piperazines. Borane-dimethylsulfide complex turned out to be the superior reagent to facilitate the transformation and delivered piperazines **76–80** with retention of configuration at the stereogenic carbon atom C6 (Scheme 7). In a final set of applications, we investigated whether biological probes could be linked to



**Scheme 7.** Reduction of various dkps to piperazines **76–80** (top) and fluorescence labelling of dkps by ligation to a coumarin probe (bottom).

chiral dkps, which in turn are specific recognition sites for enzymes.<sup>[43]</sup> A coumarin-based fluorescence label, the azide derivative of which is commercially available, was successfully ligated to the alkynyl-substituted dkps **23** and **53**. In both instances, the stereochemical integrity of the dkp was not compromised.

Our mechanistic hypothesis for the deracemization rests on the intermediacy of a selective HAT and on an enol derivative to be formed as intermediate. Although the mechanistic scenario appears similar to the pathway elucidated for hydantoin deracemization,<sup>[25]</sup> there are significant differences. Most notably, enol formation would require a return HAT to an oxygen atom that was involved in hydrogen bonding. In addition, there was no information on the feasibility of the suggested HAT to photoexcited benzophenone within complex (–)-**1**·(*R*)-dkp. Therefore, the dynamics of excited enantiopure benzophenone (–)-**1** were investigated in the absence and presence of either **47** [(*S*)-enantiomer] or *ent*-**47** [(*R*)-enantiomer] in degassed and non-degassed trifluorotoluene by transient absorption spectroscopy,<sup>[44,45]</sup> where the latter dkp enantiomer was expected to display a suitable hydrogen atom for HAT by

(*-*)-**1** (matched case) and the former does not (mismatched case).

Under ambient aerobic conditions, only the benzophenone triplet state was observed upon excitation of (*-*)-**1**, which entirely decays back into the initial ground state within less than one  $\mu\text{s}$  (Supporting Information, Figure S6.1a,d).<sup>[27]</sup> In the presence of either the mismatched substrate (*S*)-**47** or the matched substrate (*R*)-**47**, almost no triplet quenching was detected and only trace amounts of unidentified intermediates were formed (Figure S6.1a,b,c,e,f). The result is in line with the fact that a

careful exclusion of oxygen was required for the photochemical deracemization to be successful (see above). In this case, quenching by molecular oxygen is more rapid<sup>[46]</sup> than any HAT process to occur from triplet-excited benzophenone (*-*)-**1**. In the absence of molecular oxygen, the situation changed significantly as the triplet lifetime of (*-*)-**1** was extensively elongated so that bimolecular unspecific HAT between the excited triplet state and ground-state molecules occurred, yielding the protonated ketyl radical of the photocatalyst and other photoproducts with hydrogen atoms removed from the photocatalyst (Figure 1a; Support-

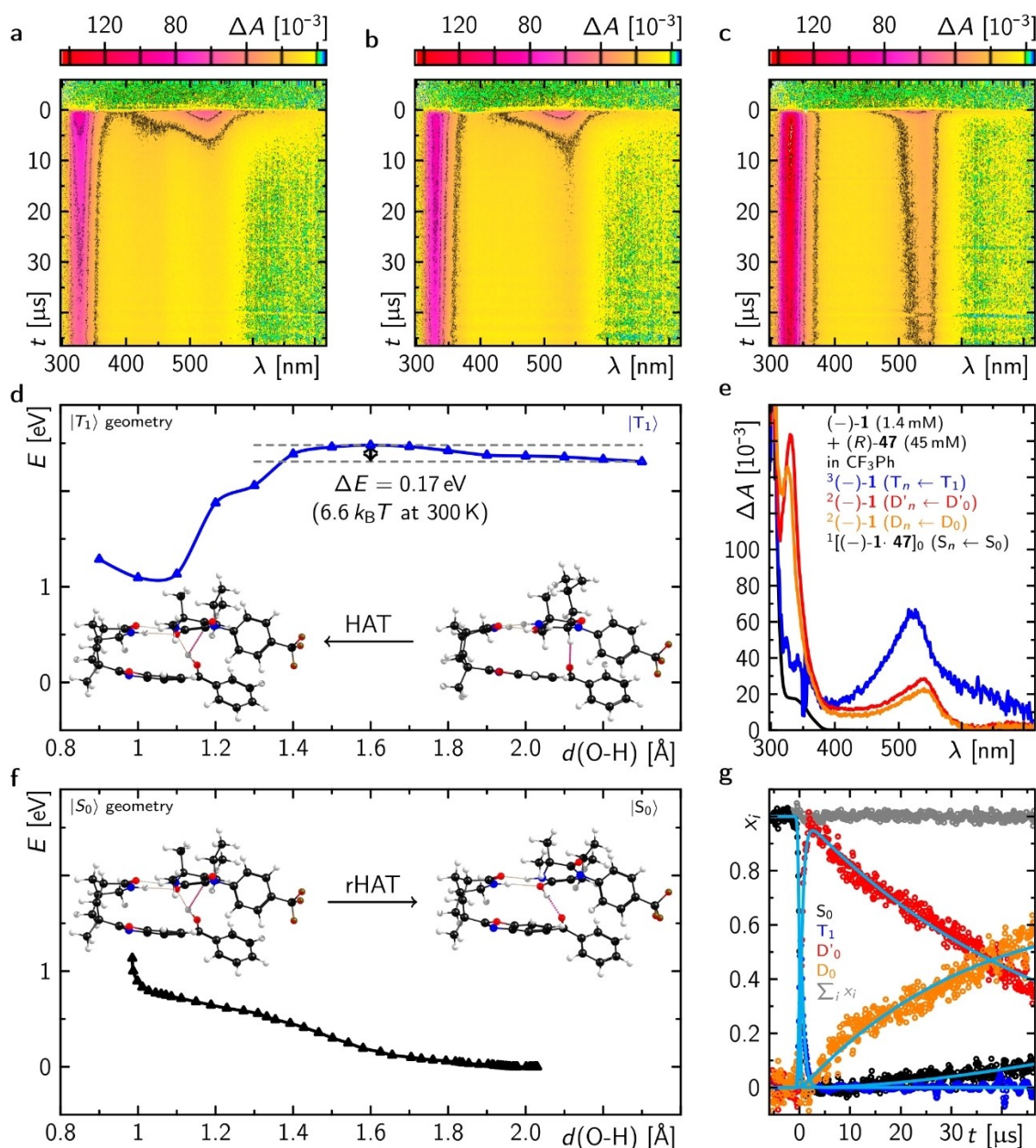


**Figure 1.** Transient absorption data of (*-*)-**1** in  $\text{PhCF}_3$  (a) and in the presence of 45 mM of either (*S*)-**47** (b) or (*R*)-**47** (c) after excitation at 355 nm in false color representation under anaerobic conditions. Species-associated spectra (e) and the corresponding mole fraction over time (together with the global fit shown in cyan; g) that contribute to the data in (c). (d and f): Potential energy surfaces for forward (d) and reverse (f) HAT in the triplet and singlet spin state, respectively. The latter was obtained by optimization of the structure in the singlet domain starting from the triplet radical pair after HAT.

ing Information: Figures S6.2a,d and S6.3a,d).<sup>[32,47]</sup> The triplet quenching occurred on two time scales as indicated by two decay-associated difference spectra (DADS) found in the global fit (see Supporting Information for further details) that showed positive (decaying) spectral features of the benzophenone triplet state. Accordingly, this may be interpreted as HAT from a  $(-)\text{-}\mathbf{1}\cdot(-)\text{-}\mathbf{1}$  complex on the order of 270 ns [black DADS in Figure S6.2d; see also Figure S7.1 for a potential  $(-)\text{-}\mathbf{1}\cdot(-)\text{-}\mathbf{1}$  complex] and from a diffusion-controlled reaction on the order of 4  $\mu\text{s}$  (blue DADS in Figure S6.2d). The protonated ketyl radical and the unidentified photoproduct(s) (broad absorption band between 400 and 450 nm) decay on a longer time scale (red DADS in Figures S6.2d and S6.3d).

Consistent with analytical data of an illuminated sample of  $(-)\text{-}\mathbf{1}$  under oxygen-free conditions, several unidentified photoproducts of  $(-)\text{-}\mathbf{1}$  were detected in the transient absorption spectra, which could not be characterized in detail. In the presence of the mismatched substrate  $(S)\text{-}\mathbf{47}$  (Figure 1b), an unspecific, bimolecular HAT occurred. In this case, a fast quenching in the sub- $\mu\text{s}$  range was not observed, which substantiates a binding of the catalyst  $(-)\text{-}\mathbf{1}$  to the mismatched substrate, blocking  $(-)\text{-}\mathbf{1}\cdot(-)\text{-}\mathbf{1}$  complex formation. The diffusion-controlled HAT is in the order of 1.6 to 10  $\mu\text{s}$  (black and red DADS in Figure S6.2e). The protonated ketyl radical and the photoproducts again decayed on a longer time scale (red DADS in Figures S6.2e and S6.3e).

In the presence of the matched substrate  $(R)\text{-}\mathbf{47}$  (Figure 1c), a clean bimolecular HAT from the triplet photocatalyst to the substrate took place with a 550 ns lifetime within complex  $(-)\text{-}\mathbf{1}\cdot(R)\text{-}\mathbf{47}$  (black DADS in Figure S6.2f showing the positive triplet decay and the negative rising of the benzophenone ketyl radical). Interestingly, on a 12  $\mu\text{s}$  time scale, small spectral changes in particular at around 340 nm were notable (blue DADS in Figure S6.2f). Such small changes may either indicate a rearrangement within complex **83** (Figure 1d) or complete dissociation of the complex leaving the free benzophenone ketyl radical as the only detectable species. In either scenario, the formed protonated ketyl radical decays on a much longer time scale (red DADS in Figures S6.2f and S6.3f). In the first scenario, reverse HAT may be hindered due to a new hydrogen bonding situation in complex **83**, i.e., a two-fold hydrogen bond of the dkp carbonyl group to the initially H-bonded N–H and the O–H of the protonated ketyl radical (see below; see also Figures 1d,f; Figure S7.2, and video Movie\_T1\_200 ps\_T1toS0\_1200 ps.mp4). In the latter scenario, reverse HAT is completely under diffusion control. For both scenarios the kinetic model is identical (see Supporting Information) and yields the well-known species-associated spectra of the triplet benzophenone and the protonated benzophenone ketyl radical (Figure 1e, where  $D_0$  and  $D'_0$  denote the ketyl radical in the initial complex and the long-lived species, respectively) with physically consistent concentration time profiles (Figure 1g).

In terms of energetic considerations, the barrier for a forward HAT within complex **83** may be estimated by quantum-chemical calculations. Within the time-dependent

density functional approximation, the forward HAT on the triplet potential surface should proceed with an activation barrier of only 0.17 eV ( $6.6 k_{\text{B}}T$  at 300 K, Figure 1d) which is accessible by thermal fluctuations. In the triplet domain, the protonated ketyl radical is further stabilized by forming an additional hydrogen bond between the carbonyl group of  $(R)\text{-}\mathbf{47}$  and the O–H bond of the benzophenone ketyl radical (Figure 1f). After intersystem crossing and formation of the singlet correlated radical pair, reverse HAT to the carbonyl group of  $(R)\text{-}\mathbf{47}$ , i.e., the carbonyl group involved in the binding between  $(-)\text{-}\mathbf{1}$  and  $(R)\text{-}\mathbf{47}$ , should immediately occur on the singlet potential surface (Figure 1f). However, in the experiment, a rapid reverse HAT was not observed and the signal of putative dkp-derived enol (see Scheme 1) could not be detected. Instead, the transient signal assigned to the protonated ketyl radical persisted for time scales  $>1$  ms. Although there is little if any precedence for a radical pair staying in a triplet correlated manifold for such a long time period, the relatively clean reaction course suggests that a slow but efficient decay to defined products occurs. As no accumulation of the enol form is detected, the data could indicate that the enol formation is much slower than its decay to the starting materials  $(S)\text{-}\mathbf{47}$  and  $(R)\text{-}\mathbf{47}$  by tautomerization.<sup>[48]</sup> An alternative pathway would involve a dissociation of the complex **83** before reverse HAT (on a  $\mu\text{s}$  time scale) and a HAT which is entirely diffusion controlled. A molecular dynamics simulation showed no rapid reverse HAT and instead the beginning of structural changes towards longer distances at the hydrogen bonding site (Figure S7.2 and video Movie\_T1\_200 ps\_T1toS0\_1200 ps.mp4).

## Conclusion

In summary, we have shown for the first time that chiral 2,5-dkps with a diverse substitution pattern can be successfully deracemized in a photocatalytic process. The absolute configuration at carbon atom C6 can be set up at will depending on the choice of catalyst, and the protocol can be used for the stereochemical editing of compounds with multiple stereogenic centers. Consecutive reactions of the products occur with retention of configuration and facilitate for example the synthesis of enantiopure *N*-aryl amino acids and of piperazines. Mechanistically, the most remarkable aspect is the fact that benzophenone catalyst **1** operates also in a scenario in which the initial HAT generates a carbon-centered radical conjugated only to the lactam entity involved in hydrogen bonding to the catalyst. In the respective complex the protonated ketyl radical forms a hydrogen bond to the oxygen atom of the lactam which implies that the back-HAT occurs to this position. While evidence for the initial HAT could be obtained by transient absorption spectroscopy, the latter hypothesis could not be corroborated and requires further studies. Still, it is evident from this work and from previous work on oxindoles<sup>[29]</sup> that deracemization does not rely on an additional carbonyl group as seen in hydantoins,<sup>[24,25]</sup> but that lactams with a



stereogenic center in  $\alpha$ -position are suited for a deracemization by reversible HAT.

### Acknowledgements

Financial support by the Deutsche Forschungsgemeinschaft (Ba 1372/23 and TRR 325; projects A5, B2; 444632635), and the Fonds der Chemischen Industrie (Kekulé fellowship to JG) is gratefully acknowledged. We thank O. Ackermann, N. Pflaum and J. Kudermann (all TU München) for their help with the HPLC and GC analysis and Dr. Stefan Breitenlechner (TU München) for helpful discussions. Open Access funding enabled and organized by Projekt DEAL.

### Conflict of Interest

The authors declare no conflict of interest.

### Data Availability Statement

The data that support the findings of this study are available in the supplementary material of this article.

**Keywords:** Amino Acids · C–H Activation · Enantioselectivity · Nitrogen Heterocycles · Photochemistry

- [1] A. Kirschning, *Chem. Eur. J.* **2022**, *28*, e202201419.
- [2] M. Quack, G. Seyfang, G. Wichmann, *Chem. Sci.* **2022**, *13*, 10598–10643.
- [3] <https://www.grandviewresearch.com/industry-analysis/amino-acids-market> accessed on September 9, 2023.
- [4] A. D. Borthwick, *Chem. Rev.* **2012**, *112*, 3641–3716.
- [5] P. Borgman, R. D. Lopez, A. L. Lane, *Org. Biomol. Chem.* **2019**, *17*, 2305–2314.
- [6] C. H. Schiwiek, C. Jandl, C. T. Bach, *ACS Catal.* **2022**, *12*, 3628–3633.
- [7] Example: J. Frenkel, C. Wess, W. Vyverman, G. Pohnert, *J. Chromatogr. B* **2014**, *951*–952, 58–61.
- [8] Review: Y. Teng, C. Gu, Z. Chen, H. Jiang, Y. Xiong, D. Liu, D. Xiao, *Chirality* **2022**, *34*, 1094–1119.
- [9] First report: A. Hözl-Hobmeier, A. Bauer, A. V. Silva, S. M. Huber, C. Bannwarth, T. Bach, *Nature* **2018**, *564*, 240–243.
- [10] Reviews: a) J. Großkopf, T. Bach, *Angew. Chem. Int. Ed.* **2023**, *62*, e202308241; b) J. Wang, X. Lv, Z. Jiang, *Chem. Eur. J.* **2023**, *29*, e202204029; c) Y. Su, Y. Zou, W. Xiao, *Chin. J. Org. Chem.* **2022**, *42*, 3201–3212; d) Q. Shi, J. Ye, *Angew. Chem. Int. Ed.* **2020**, *59*, 4998–5001; e) C. Yang, Y. Inoue, *Nature* **2018**, *564*, 197–199.
- [11] General reviews including photochemical deracemization: a) M. Huang, T. Pan, X. Jiang, S. Luo, *J. Am. Chem. Soc.* **2023**, *145*, 10917–10929; b) P.-Z. Wang, W.-J. Xiao, J.-R. Chen, *Nat. Chem. Rev.* **2023**, *7*, 35–50; c) J. S. DeHovitz, T. K. Hyster, *ACS Catal.* **2022**, *12*, 8911–8924.
- [12] D. G. Blackmond, *Angew. Chem. Int. Ed.* **2009**, *48*, 2648–2654.
- [13] a) C. Aranda, G. Oksdath-Mansilla, F. R. Bisogno, G. de Gonzalo, *Adv. Synth. Catal.* **2020**, *362*, 1233–1257; b) M. Rachwal-ski, N. Vermue, F. P. J. T. Rutjes, *Chem. Soc. Rev.* **2013**, *42*, 9268–9282.
- [14] For general reviews on enantioselective photochemical reactions, see: a) M. J. Genzink, J. B. Kidd, W. B. Swords, T. P. Yoon, *Chem. Rev.* **2022**, *122*, 1654–1716; b) C. Prentice, J. Morrisson, A. D. Smith, E. Zysman-Colman, *Beilstein J. Org. Chem.* **2020**, *16*, 2363–2441; c) M. Silvi, P. Melchiorre, *Nature* **2018**, *554*, 41–49.
- [15] L. Wimberger, T. Kratz, T. Bach, *Synthesis* **2019**, *51*, 4417–4424.
- [16] X. Li, R. J. Kutta, C. Jandl, A. Bauer, P. Nuernberger, T. Bach, *Angew. Chem. Int. Ed.* **2020**, *59*, 21640–21647.
- [17] M. Plaza, J. Großkopf, S. Breitenlechner, C. Bannwarth, T. Bach, *J. Am. Chem. Soc.* **2021**, *143*, 11209–11217.
- [18] T. Kratz, P. Steinbach, S. Breitenlechner, G. Storch, C. Bannwarth, T. Bach, *J. Am. Chem. Soc.* **2022**, *144*, 10133–10138.
- [19] C. Zhang, A. Z. Gao, X. Nie, C.-X. Ye, S. I. Ivlev, S. Chen, E. Meggers, *J. Am. Chem. Soc.* **2021**, *143*, 13393–13400.
- [20] M. Huang, L. Zhang, T. Pan, S. Luo, *Science* **2022**, *375*, 869–874.
- [21] Z. Gu, L. Zhang, H. Li, S. Cao, Y. Yin, X. Zhao, X. Ban, Z. Jiang, *Angew. Chem. Int. Ed.* **2022**, *61*, e202211241.
- [22] C. Onneken, T. Morack, J. Soika, O. Sokolova, N. Niemeyer, C. Mück-Lichtenfeld, C. G. Daniliuc, J. Neugebauer, R. Gilmour, *Nature* **2023**, *621*, 753–759.
- [23] N. Y. Shin, J. M. Ryss, X. Zhang, S. J. Miller, R. R. Knowles, *Science* **2019**, *366*, 364–369.
- [24] J. Großkopf, M. Plaza, A. Seitz, S. Breitenlechner, G. Storch, T. Bach, *J. Am. Chem. Soc.* **2021**, *143*, 21241–21245.
- [25] R. J. Kutta, J. Großkopf, N. van Staaldunin, A. Seitz, P. Pracht, S. Breitenlechner, C. Bannwarth, P. Nuernberger, T. Bach, *J. Am. Chem. Soc.* **2023**, *145*, 2354–2363.
- [26] A. Dömling, I. Ugi, *Angew. Chem. Int. Ed.* **2000**, *39*, 3168–3210.
- [27] G. Dormán, H. Nakamura, A. Pulsipher, G. D. Prestwich, *Chem. Rev.* **2016**, *116*, 15284–15398.
- [28] J. R. Lancaster, R. Smilowitz, N. J. Turro, J. T. Koberstein, *Photochem. Photobiol.* **2014**, *90*, 394–401.
- [29] J. Großkopf, A. A. Heidecker, T. Bach, *Angew. Chem. Int. Ed.* **2023**, *62*, e202305274.
- [30] M. Pettersson, M. Quant, J. Min, L. Inconaru, R. W. Kriwacki, M. B. Waddell, R. K. Guy, K. Luthman, M. Grøtli, *PLoS One* **2015**, *10*, e0124423.
- [31] Y.-R. Luo, *Handbook of Bond Dissociation Energies in Organic Compounds*; CRC Press, Boca Raton, **2003**.
- [32] A. V. Buettner, J. Dedinas, *J. Phys. Chem.* **1971**, *75*, 187–191.
- [33] Y. Wang, H. M. Carder, A. E. Wendlandt, *Nature* **2020**, *578*, 403–408.
- [34] C. J. Oswood, D. W. C. MacMillan, *J. Am. Chem. Soc.* **2022**, *144*, 93–98.
- [35] Y.-A. Zhang, X. Gu, A. E. Wendlandt, *J. Am. Chem. Soc.* **2022**, *144*, 599–605.
- [36] A. M. Kazerouni, D. S. Brandes, C. C. Davies, L. F. Cotter, J. M. Mayer, S. Chen, J. A. Ellman, *ACS Catal.* **2022**, *12*, 7798–7803.
- [37] H. M. Carder, Y. Wang, A. E. Wendlandt, *J. Am. Chem. Soc.* **2022**, *144*, 11870–11877.
- [38] Y.-A. Zhang, V. Palani, A. E. Seim, Y. Wang, K. J. Wang, A. E. Wendlandt, *Science* **2022**, *378*, 383–390.
- [39] For a definition of the *rac/ent*-nomenclature, see: G. Quinkert, H. Stark, *Angew. Chem. Int. Ed.* **1983**, *22*, 637–655.
- [40] S. M. King, S. L. Buchwald, *Org. Lett.* **2016**, *18*, 4128–4131.
- [41] J. Jampílek, R. Opratřilová, A. Řezáčová, Z. Oktábec, J. Dohnal, WO 2014 019556 A1, **2012**.
- [42] S. D. J. Magnan, F. N. Shirota, H. T. Nagasawa, *J. Med. Chem.* **1982**, *25*, 1018–1021.
- [43] Z. Tian, Y. Chu, H. Wang, L. Zhong, M. Deng, W. Li, *RSC Adv.* **2018**, *8*, 1055–1064.

- [44] R. J. Kutta, T. Langenbacher, U. Kensity, B. Dick, *Appl. Phys. B* **2013**, *111*, 203–216.
- [45] R. J. Kutta, U. Kensity, B. Dick, in *Chemical Photocatalysis* (Ed. B. König) De Gruyter, Berlin, **2013**, pp. 295–318.
- [46] S. K. Chattopadhyay, C. V. Kumar, P. K. Das, *J. Photochem.* **1985**, *30*, 81–91.
- [47] T. S. Godfrey, W. Hilpern, G. Porter, *Chem. Phys. Lett.* **1967**, *1*, 490–492.
- [48] B. Bandyopadhyay, P. Pandey, P. Banerjee, A. K. Samanta, T. Chakraborty, *J. Phys. Chem. A* **2012**, *116*, 3836–3845.

Manuscript received: September 13, 2023

Accepted manuscript online: October 4, 2023

Version of record online: October 4, 2023